Electronic Supplementary Material (ESI) for Green Chemistry.

Paired Electrolysis of 5-(Hydroxymethyl)furfural in Flow Cells with High-Performance Oxide-Derived Silver Cathode

Hengzhou Liu,[a] Ting-Han Lee,[a] Yifu Chen,[a] Eric W. Cochran,[a*] Wenzhen Li[a*]

[a] *Department of Chemical and Biological Engineering, Iowa State University, 618 Bissell Road, Ames, Iowa, 50011, United States*

Corresponding authors: W. Li (wzli@iastate.edu), E. W. Cochran (ecochran@iastate.edu)

Supplementary Figures and Tables

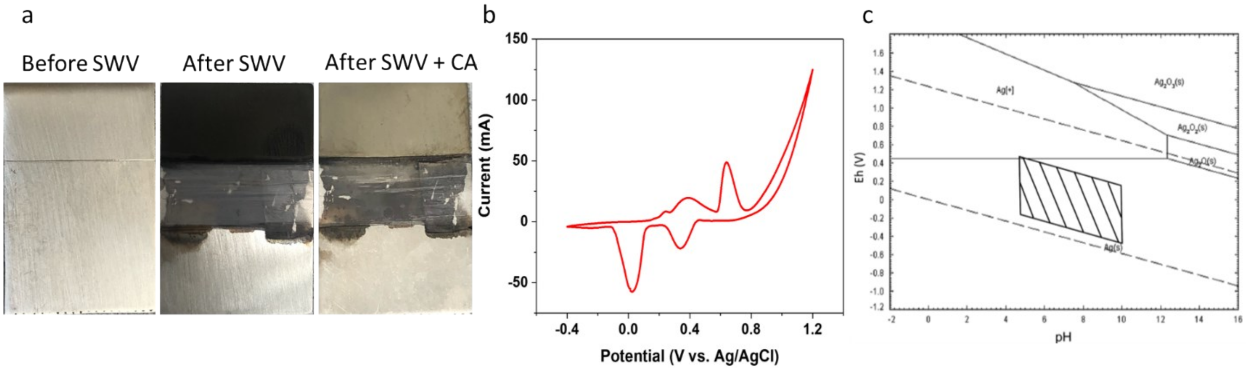

Fig. S1. (a) Photographs of Ag foil before the SWV treatment, after the SWV treatment, and after the SWV treatment followed by CA. (b) Cyclic voltammogram of Ag foil in 0.2 M NaOH with a scan rate of 20 mV s^{-1}. (c) Pourbaix diagram of Ag showing its thermodynamically favorable species as function of potential E_h and pH.[1]

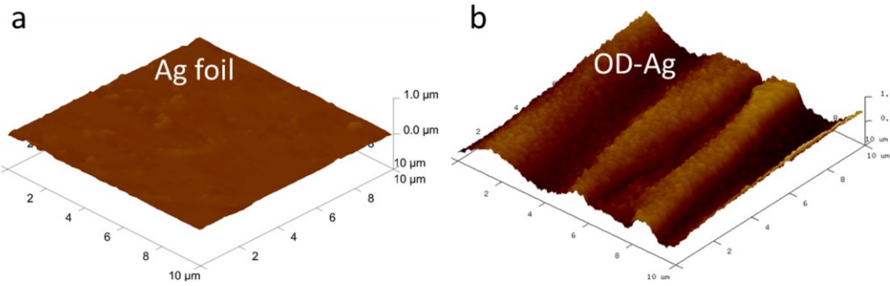

Fig. S2. AFM 3D images of (a) Ag foil and (b) OD-Ag with a 10 × 10 µm surface area.

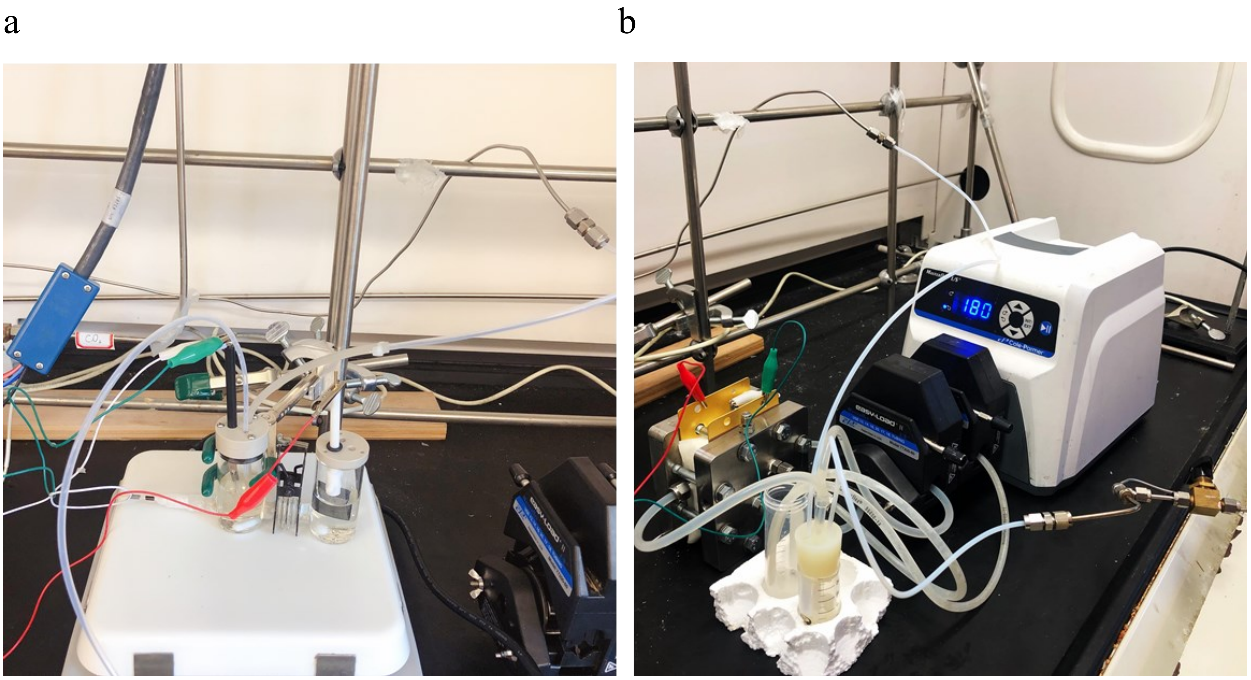

Fig. S3. Experimental setup of the paired electrolytic system. Photograph of (a) the H-type cell and (b) the flow cell.

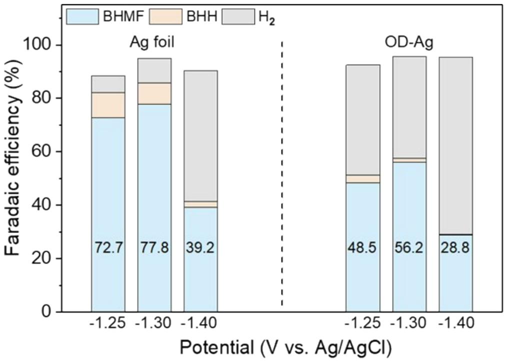

Fig. S4. Faradaic efficiency of different products from ECH of 20 mM HMF in 0.5 M borate buffer (pH 9.2) on Ag foil (left columns) and OD-Ag (right columns) at different applied potentials for half-hour electrolysis.

Calculation of energy efficiency

The Gibbs free energy can be converted to standard equilibrium potential (*vs.* SHE) by Eqn S1:

$$\Delta G^\circ = -nFE^\circ \tag{S1}$$

Where ΔG° (kJ mol^{-1}) is the Gibbs free energy; n is the number of electrons transferred; F is the Faraday constant (96,485 C mol^{-1}); E^0 is the standard redox potential of the corresponding redox couples versus the standard hydrogen electrode (SHE).

Nernst equation was used for the calculation of thermodynamic potential by Eqn. S2:

$$E = E^\circ - 0.059 \times pH \tag{S2}$$

The two half-reactions, the overall paired reaction, and the thermodynamic potentials are shown in Eqs. S3–5:

$$\text{Cathode: } 3HMF + 6H^+ + 6e^- \longrightarrow 3BHMF \qquad E^\circ = 0.120\ V\ (vs. SHE) \tag{S3}$$

$$\text{Anode: } HMF + 2H_2O \longrightarrow FDCA + 6H^+ + 6e^- \quad E^\circ = -0.450\ V\ (vs. SHE) \tag{S4}$$

$$\text{Overall: } 4HMF + 2H_2O \longrightarrow 3BHMF + FDCA \quad E^\circ = -0.330\ V\ (vs. SHE) \tag{S5}$$

The standard potentials (E^0) for HMF-to-BHMF and HMF-to-FDCA reactions are obtained from the literature.[2]

Energy efficiency (ε) as a function of cell voltage (V_{cell}) can be calculated by Eqn. S6:

$$\varepsilon = \frac{|E_{cell}|}{V_{cell}} = \frac{|FE_{\text{BHMF}} \cdot E_{HMF/BHMF} - FE_{\text{FDCA}} \cdot E_{HMF/FDCA}|}{V_{cell}} \times 200\% \tag{S6}$$

Noted that the electrons are transferred from the HMF at anode to the HMF at cathode, so the maximum combined FE is 200%.

Table S1. Summary of the cell voltage[a] and faradaic efficiencies (FE) for HMF paired electrolysis in H-type cell and flow cell.

Time	Average cell voltage (V, flow cell)	BHMF FE in flow cell (%)	FDCA FE in flow cell (%)	Average cell voltage (V, H-type cell)	BHMF FE in H-type cell (%)	FDCA FE in flow cell (%)
1st hour	2.0	80.4	83.4	7.4	74.9	99.7
2nd hour	2.1	78.9		7.7	71.4	
3rd hour	2.3	80.9		7.8	74.7	

a. The cell voltages are obtained from Fig. 5a.

Calculation of ε in the flow cell as an example:

In pH 9.2 buffer solution:

Reduction of HMF to BHMF: $E = 0.120 - 0.059 \times 9.2 = -0.4228$ V

Reduction of FDCA to HMF: $E = 0.450 - 0.059 \times 9.2 = -0.0928$ V

1st hour:

$$\varepsilon = \frac{|E_{cell}|}{V_{cell}} = \frac{|FE_{\mathrm{BHMF}} \times E_{HMF/BHMF} - FE_{\mathrm{FDCA}} \times E_{HMF/FDCA}|}{V_{cell}} \times 200\% = \frac{|0.804 \times (-0.4228) - 0.834}{2.0}$$

$$\times 200\% = 26.2\%$$

2nd hour:

$$\varepsilon = \frac{|0.789 \times (-0.4228) - 0.834 \times (-0.0928)|}{2.1} \times 200\% = 24.4\%$$

3rd hour

$$\varepsilon = \frac{|0.809 \times (-0.4228) - 0.834 \times (-0.0928)|}{2.3} \times 200\% = 23.0\%$$

Average ε for 3-hour electrolysis:

$$\varepsilon = \frac{26.2\% + 24.4\% + 23.0\%}{3} = 24.5\%$$

Similarly, the calculated ε for the H-type cell measurement is 5.7%.

Calculation of electricity consumption for BHMF and FDCA production

The data for calculation are obtained from Table S1.

At the current of 10 mA in the flow cell:

1st hour:

Electricity consumption: $W_1 = U \times I \times t = 2.0\ \text{V} \times 0.01\ \text{A} \times 3600\ \text{s} = 2.0\ \text{V} \times 0.01\ \text{A} \times 1\ \text{h} = 0.02\ \text{Wh}$

Produced BHMF: $m_{\text{BHMF}} = \dfrac{I \times t \times FE \times M_{BHMF}}{2F} = 0.019\ \text{g}$

Where U is the cell voltage (V), I is the current (A), t is the reaction time (s), FE is the faradaic efficiency of BHMF, M_{BHMF} is the molar mass of BHMF (128 g mol^{-1}), and F is the Faraday constant (96,485 C mol^{-1}).

2nd hour: $W_2 = U \times I \times t = 2.1\ \text{V} \times 0.01\ \text{A} \times 1\ \text{h} = 0.021\ \text{Wh}$

$m_{\text{BHMF}} = 0.019\ \text{g}$

3rd hour: $W_3 = U \times I \times t = 2.3\ \text{V} \times 0.01\ \text{A} \times 1\ \text{h} = 0.023\ \text{Wh}$

$m_{\text{BHMF}} = 0.019\ \text{g}$

Total electricity consumption: $W_t = 0.064\ \text{Wh}$

Total mass: $m_{\text{BHMF}} = 0.057\ \text{g}$

Similarly, total mass: $m_{\text{FDCA}} = 0.024\ \text{g}$

Thus, the energy consumption normalized by the mass of products (in kWh kg^{-1}) in the flow cell:

BHMF: 0.064/0.057 = 1.12 kWh kg^{-1}

FDCA: 0.064/0.024 = 2.64 kWh kg^{-1}

Similarly, in the H-type cell:

BHMF: 0.064/0.024 = 2.64 kWh kg^{-1}

FDCA: 0.229/0.029 = 7.89 kWh kg^{-1}

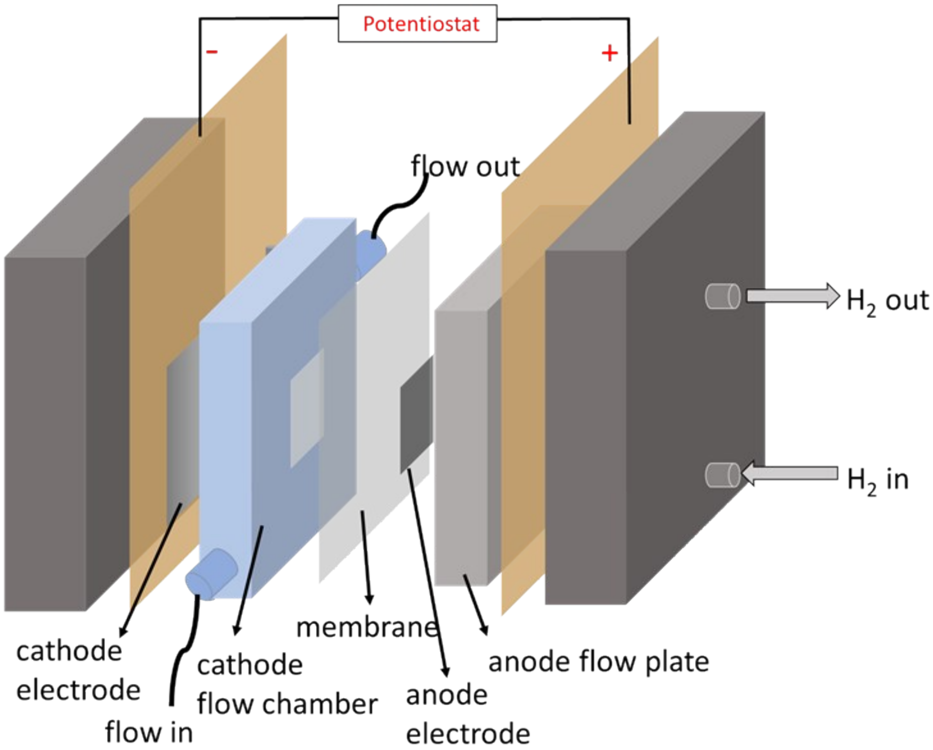

Fig. S5. The flow cell configuration of HMF paired electrolysis for linear sweep voltammetry and constant current (10 mA) measurements.

Table S2. Summary of results obtained from TEMPO-mediated ECO of HMF to FDCA in the H-type cell.[a]

Potential ($V_{Ag/AgCl}$)	**Current (mA)**	**Applied charge (C)**	**HMF conversion (%)**	**FDCA selectivity (%)**	**FDCA faradaic efficiency (%)**
0.4	N/A	57.9	100	94.3	93.7
0.6	N/A		100	97.1	96.5
0.7	N/A		100	94.0	93.4
0.8	N/A		100	96.4	95.9
N/A	10		100	98.3	97.2

a. TEMPO-mediated HMF oxidation was performed in 20 ml of 0.5 M borate buffer (pH 9.2) with 5 mM HMF and 7.5 mM TEMPO at constant potential or constant current conditions. The applied charge was 57.9 C, corresponding to the theoretical charge required for 100% conversion of HMF to FDCA (0.005 M × 0.02 L × 6 × 96485 C mol^{-1} = 57.9 C).

Table S3. Cathodic results of paired electrolysis in the H-type cell at 10 mA.[a]

Batch	Time (h)	Conversion (%)	BHMF selectivity (%)	BHMF FE (%)	BHH selectivity (%)	BHH FE (%)
1	1	39.7	87.5	74.9	9.8	4.1
2	1	37.4	88.9	71.4	8.1	3.2
3	1	36.9	87.2	74.7	6.6	2.4
Average[b]		38.0	87.9	73.7	8.2	3.2
Standard dev.[b]		1.5	0.9	2.0	1.6	0.9
4	0.2	7.4	92.0	73.6	4.7	1.6

Table S4. Anodic results of paired electrolysis in the H-type cell at 10 mA.[a]

Conversion (%)	FDCA selectivity (%)	FDCA FE (%)
100	100.4	99.7

a. The catholyte was 20 ml of 0.5 M borate buffer (pH 9.2) with 20 mM HMF, and the anolyte was 20 ml of 0.5 M borate buffer (pH 9.2) with 10 mM HMF and 7.5 mM TEMPO. The applied charge for H-type cell test was 116 C (the total reaction time was 3.2 h), corresponding to the theoretical charge required for 100% conversion of HMF to FDCA. Fresh catholyte was replaced every hour during tests.

b. The average value and standard deviation were calculated based on three consecutive 1-hour measurements.

Table S5. Cathodic results of paired electrolysis in the flow cell at 10 mA.[a]

Batch	Time (h)	Conversion (%)	BHMF selectivity (%)	BHMF FE (%)	BHH selectivity (%)	BHH FE (%)
1	1	41.8	90.0	80.4	7.0	3.1
2	1	38.9	88.2	78.9	5.4	2.0
3	1	40.1	89.6	80.9	5.1	1.9
Average[b]		40.3	89.3	80.1	5.8	2.3
Standard Dev.[b]		1.5	0.9	1.1	1.0	0.7
4	0.8	32.8	89.2	80.6	3.8	1.8

Table S6. Anodic results of paired electrolysis in the flow cell at 10 mA.[a]

Conversion (%)	FDCA selectivity (%)	FDCA FE (%)
100	98.8	83.4

a. The catholyte was 20 ml of 0.5 M borate buffer (pH 9.2) with 20 mM HMF, and the anolyte was 20 ml of 0.5 M borate buffer (pH 9.2) with 10 mM HMF and 7.5 mM TEMPO. The applied charge for H-type cell test was 136 C (the total reaction time was 3.8 h), corresponding to the theoretical charge required for 100% conversion of HMF to FDCA. Fresh catholyte was replaced every hour during tests.

b. The average and standard deviation were calculated based on three consecutive 1-hour measurements.

Table S7. Solution resistance determined by potentiostatic electrochemical impedance spectroscopy (EIS).

Cell type	Resistance between the working and reference electrodes (Ω)	Resistance between the working and counter electrodes (Ω)
H-type cell	27.9	491.2
flow cell	19.2	39.8

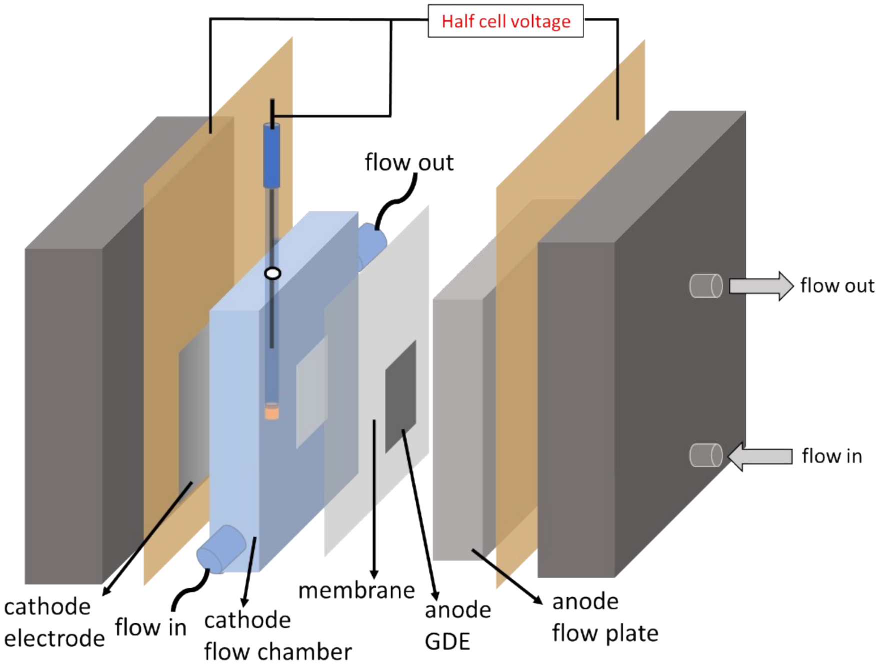

Fig. S6. The flow cell configuration for HMF paired electrolysis at the constant potential of 0.6 $V_{Ag/AgCl}$ between the reference electrode and anode. The cell voltage between the working electrode and anode was monitored by a multimeter.

Table S8. Cathodic results of paired electrolysis at the constant potential of 0.6 $V_{Ag/AgCl}$ between the reference electrode and anode.

Cell type	Reaction time (min)	Conversion (%)	BHMF selectivity (%)	BHMF FE (%)	BHH selectivity (%)	BHH FE (%)
H-type cell	120	69.0	78.2	74.0	18.6	8.8
flow cell	85	41.4	86.1	60.5	8.2	2.9

Table S9. Anodic results of paired electrolysis at the constant potential of 0.6 $V_{Ag/AgCl}$ between the reference electrode and anode.

Cell	Reaction time (min)	Conversion (%)	BHMF selectivity (%)	BHMF FE (%)	BHH selectivity (%)	BHH FE (%)
H-type cell	120	100	97.1	96.5	2.1	1.2
flow cell	85	100	94.0	92.7	4.1	2.7

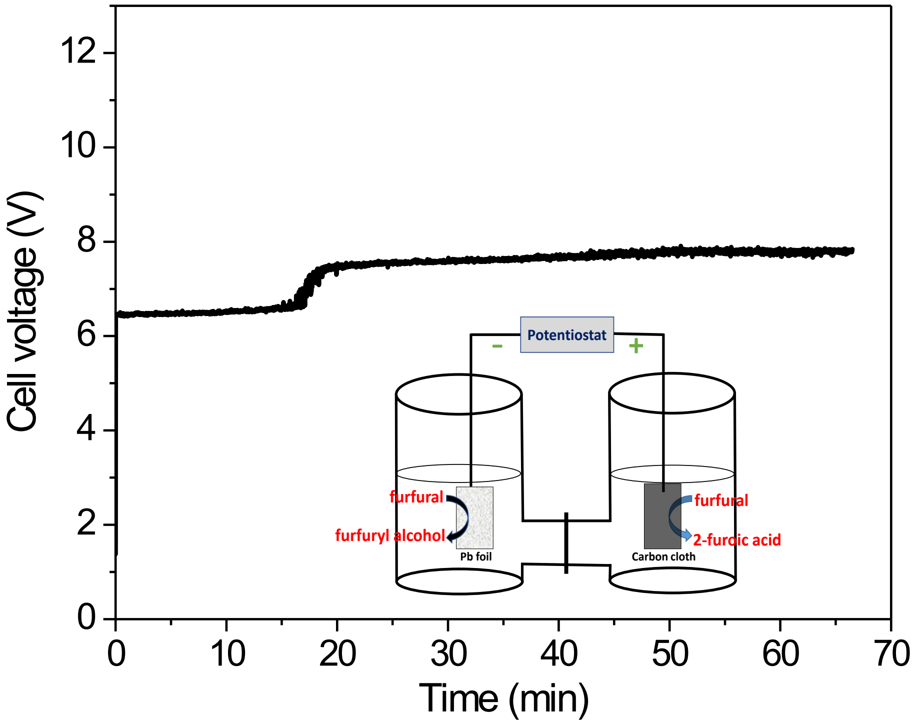

Fig. S7. Paired electrolysis of furfural in the H-type cell at 10 mA. The catholyte was 20 ml of 0.1 M phosphate buffer (pH 7) in 25/75 (v/v) CH_3CN/H_2O solvent with 10 mM furfural, and the anolyte was 0.1 M phosphate buffer (pH 7) in 25/75 (v/v) CH_3CN/H_2O with 10 mM furfural and 7.5 mM TEMPO. Pb foil and carbon cloth were used as the cathode and anode, respectively. The applied charge for paired electrolysis was 40 C (theoretical charge for 100% conversion of furfural at anode is 38.6 C).

Table S10. Results of furfural paired electrolysis at the cathode.

Conversion (%)	FA selectivity (%)	FA FE (%)	Hydrofuroin selectivity (%)	Hydrofuroin FE (%)
56.8	82.5	90.6	10.1	5.5

Table S11. Results of furfural paired electrolysis at the anode.

Conversion (%)	2-furoic acid selectivity (%)	2-furoic acid FE (%)
89.4	98.0	87.2

Paired electrolysis	**C (mM)**[a]	**Conditions**	**Reactor**	**Cathode**	**Anode**	**Cathode FE (%)**	**Anode FE (%)**	**ε (%)**[b]	**Ref.**
HMF-HMF	10	0.5 M borate buffer (pH 9.2)	H-type cell	Ag/C	Carbon felt (TEMPO-mediated)	85	98	N/A	[3]
p-nitrophenol-HMF	10	1.0 M KOH	H-type cell	NiBx@NF	NiBx@NF	>99	>99	N/A	[4]
HMF-HMF	10	0.2 M $HClO_4$	Flow cell	Pd/VN	3D VN	≥86	≥84	N/A	[5]
Furfural-Furfural	50	1.0 M KOH	H-type cell	Cu_3P/CFC	Ni_2P/CFC	92.0–98.0	90.0–98.0	N/A	[6]
benzonitrile derivatives-tertiary amines	0.4	nBu_4NClO_4, 1,4-lutidine and DMA mixture	One-compartment electrolytic cell	RVC	RVC (TEMPO-mediated)	N/A	N/A	N/A	[7]
ketones-benzylic alcohols	25	0.1 M nBu_4NOAc (CH_3CN/EtOAc = 3/7)	One-compartment electrolytic cell	Ni	graphite	N/A	N/A	N/A	[8]
Nitrobenzene-aryl-sulfinic acids	1.0	0.2 M phosphate buffer (pH 3.5)	One-compartment electrolytic cell	Glassy carbon	Glassy carbon	N/A	N/A	N/A	[9]
benzylic C–H bond convergent paired	0.6	0.1 M $LutHClO_4$	One-compartment electrolytic cell	Carbon fiber	FTO	N/A	N/A	N/A	[10]
CO_2-HMF	10	0.5 M $KHCO_3$	H-type cell	NiO NP_s	BiO_x	81	36	N/A	[11]
CO_2-methanol	1000	1.0 M $KHCO_3$ 1.0 M KOH[c]	H-type cell	$mSnO_2$/CC	CuONS/CF	80.5	91.3	N/A	[12]
CO_2-glycerol	50	0.5 M $KHCO_3$	H-type cell	CP|CNT-CoPPc	mesoITO/STEMPO	82	83	18	[13]
CO_2-benzyl alcohol	100	0.5 M Na_2SO_4 (pH 7.2); 0.5 M acetate buffer (pH 5)[d]	H-type cell	Ru-based	Ru-based	30-40	~70	17.6	[14]
CO_2-1,2-Propanediol	20	0.5 M $KHCO_3$	Microflow cell	Au/C	Carbon felt (TEMPO mediated)	76	80	N/A	[15]
CO_2-alcohols	0.25	0.5 M $NaHCO_3$	One-compartment electrolytic cell	Cu-In film	Pt mesh (TEMPO mediated)	>70	>75	N/A	[16]
CO_2-glycerol	2000	2.0 M KOH	Flow cell	Ag NPs	IrO_2	N/A	N/A	N/A	[17]
H_2O-HMF	10	1.0 M KOH	H-type cell	Ni_3S_2/NF	Ni_3S_2/NF	~100	98	N/A	[18]
CO_2- NH_3	10	5.0 M KOH	H-type cell and flow cell	Deposited Ag	Pt/C	90	N/A	N/A	[19]
HMF-HMF	20	0.5 M borate buffer (pH 9.2)	Flow cell	OD-Ag	Carbon cloth (TEMPO-mediated)	80.9	83.4	24.5	This work
HMF-H_2	20	0.5 M borate buffer (pH 9.2)	Flow cell	OD-Ag	Pt/C	82.3	N/A	N/A	This work

Table S12. Summary of recently demonstrated paired electrolysis systems.

a. concentration of organic feedstock. b. energy efficiency c. 1.0 M $KHCO_3$ and 1.0 M KOH as the electrolyte for the cathode and cathode compartment, respectively. d. 0.5 M Na_2SO_4 (pH 7.2) and 0.5 M acetate buffer (pH 5) as electrolytes for the cathode and cathode compartment, respectively.

References

1. M. Hans, S. Mathews, F. Mücklich and M. Solioz, *Biointerphases*, 2016, **11**, 018902.
2. Y. Kwon, K. J. P. Schouten, J. C. van der Waal, E. de Jong and M. T. Koper, *ACS Catal.*, 2016, **6**, 6704-6717.
3. X. H. Chadderdon, D. J. Chadderdon, T. Pfennig, B. H. Shanks and W. Li, *Green Chem.*, 2019, **21**, 6210-6219.
4. P. Zhang, X. Sheng, X. Chen, Z. Fang, J. Jiang, M. Wang, F. Li, L. Fan, Y. Ren and B. Zhang, *Angew. Chem. Int. Ed.*, 2019, **58**, 9155-9159.
5. S. Li, X. Sun, Z. Yao, X. Zhong, Y. Cao, Y. Liang, Z. Wei, S. Deng, G. Zhuang and X. Li, *Adv. Funct. Mater.*, 2019, **29**, 1904780.
6. X. Zhang, M. Han, G. Liu, G. Wang, Y. Zhang, H. Zhang and H. Zhao, *Appl. Catal. **B***, 2019, **244**, 899-908.
7. Y. Ma, X. Yao, L. Zhang, P. Ni, R. Cheng and J. Ye, *Angew. Chem.*, 2019, **131**, 16700-16704.
8. S. Zhang, L. Li, J. Li, J. Shi, K. Xu, W. Gao, L. Zong, G. Li and M. Findlater, *Angew. Chem.*, 2021, **60**, 7275-7282.
9. B. Mokhtari, D. Nematollahi and H. Salehzadeh, *Green Chem.*, 2018, **20**, 1499-1505.
10. L. Zhang and X. Hu, *Chem. Sci.*, 2020, **11**, 10786-10791.
11. S. Choi, M. Balamurugan, K.-G. Lee, K. H. Cho, S. Park, H. Seo and K. T. Nam, *J. Phys. Chem. Lett.*, 2020, **11**, 2941-2948.
12. X. Wei, Y. Li, L. Chen and J. Shi, *Angew. Chem. Int. Ed.*, 2021, **60**, 3148-3155.
13. M. A. Bajada, S. Roy, J. Warnan, K. Abdiaziz, A. Wagner, M. M. Roessler and E. Reisner, *Angew. Chem.*, 2020, **132**, 15763-15771.
14. Y. Wang, S. Gonell, U. R. Mathiyazhagan, Y. Liu, D. Wang, A. J. Miller and T. J. Meyer, *ACS Appl. Energy Mater.*, 2018, **2**, 97-101.
15. E. Pérez-Gallent, S. Turk, R. Latsuzbaia, R. Bhardwaj, A. Anastasopol, F. Sastre-Calabuig, A. C. Garcia, E. Giling and E. Goetheer, *Ind. Eng. Chem. Res.*, 2019, **58**, 6195-6202.
16. T. Li, Y. Cao, J. He and C. P. Berlinguette, *ACS Cent. Sci.*, 2017, **3**, 778-783.
17. S. Verma, S. Lu and P. J. Kenis, *Nat. Energy*, 2019, **4**, 466-474.
18. B. You, X. Liu, N. Jiang and Y. Sun, *J. Am. Chem. Soc.*, 2016, **138**, 13639-13646.
19. X. V. Medvedeva, J. J. Medvedev, S. W. Tatarchuk, R. M. Choueiri and A. Klinkova, *Green Chem.*, 2020, **22**, 4456-4462.